

Adapting to Flexibility: Model Reference Adaptive Control of Soft Bending Actuators

Erik H. Skorina, Ming Luo, Weijia Tao, Fuchen Chen, Jie Fu, and Cagdas D. Onal

Abstract—Soft pneumatic actuators enable robots to interact safely with complex environments, but often suffer from imprecise control and unpredictable dynamics. This article addresses these challenges through the use of model reference adaptive control, which modulates the input to the plant to ensure that it behaves similarly to a reference dynamic model. We use adaptive control to standardize the performance of soft actuators and eliminate their non-linear behavior. We implement an adaptive controller chosen for its simplicity and efficiency, and study the ability of this controller to force different soft pneumatic actuators to behave uniformly under a variety of conditions. Next, we formulate an inverse dynamic feedforward controller, allowing soft actuators to quickly follow reference trajectories. We test the performance of the proposed feedforward controller with and without the adaptive controller, to study its open-loop effectiveness and highlight the improvements the adaptive controller offers. Our experimental results indicate that soft actuators can follow unstructured continuous signals through the use of the proposed adaptive control approach.

Index Terms—Soft Material Robotics; Robust/Adaptive Control of Robotic Systems; Hydraulic/Pneumatic Actuators

I. INTRODUCTION

SOFT pneumatic robotics [1]–[7] has many benefits over traditional robotics. It allows robots to be inherently compliant, making them safer to physically interact with the environment. This allows soft robots to operate in collaboration with humans or navigate unstructured environments without worrying about the effects of a collision.

However, the control of fully soft pneumatic robots represents a difficult engineering problem [8]. One important issue is the significant variation exhibited in soft materials. The same material can exhibit different static and dynamic properties due to uncertainties in fabrication [9], leading to unpredictability in soft robotic behavior. In addition, the dynamics of soft pneumatic actuators is nonlinear and

involves inherent and varying time delays as pressurized air flows from the source to the expansion chamber [10].

Controlling the pressure inside soft actuators remains a challenge. Air flow can be controlled using analog pneumatic cylinders [3], which are effective but bulky and expensive, prohibiting their use in a mobile robot with multiple degrees of freedom. As an alternative, an approximation of pressure control can be achieved with binary solenoid valves using a pulse width modulation (PWM) signal [11], [12], while two independently-controlled solenoid valves can be used to allow the system to also latch all air flow to maintain constant pressures inside the soft actuator [7], [13], [14]. These methods are less capable than the pneumatic cylinder method, but are more conducive to use in mobile robots.

Using PWM valve commands, a nested gain-scheduled proportional-integral-derivative (PID) controller was presented in [11], where the outer loop controls position (bending curvature) and the inner loop controls the pressure required to reach the desired position, despite with relatively slow response times. A bang-bang control was presented in [13] with a variable dead-zone depending on the desired angle. This allowed rapid signal tracking, despite with a series of spikes and staircase patterns in tracking error due to the dead-zone. In our earlier work, we employed the same PWM method for a more advanced iterative sliding mode controller on a soft actuated robotic joint [12], where we used the valve duty cycle as the control input and the joint angle for feedback. More recently, we updated this motion control approach using a direct sliding mode controller that regulates binary valve commands [7], resulting in rapid signal tracking with minimal overshoot, while in [15] we used a simpler bang-bang controller, but focus on the dynamics of the entire body of a soft robotic snake composed of multiple bending segments in series.

Our work in motion control of soft actuators revealed that these systems exhibit significant variations in dynamic response between prototypes. Model reference adaptive control [16] (MRAC) is a general control strategy that has been used on a variety of systems to ensure repeatable operation. MRAC uses a dynamic model as a reference for the desired behavior of the plant. It compares the behavior of the plant and that of the model and modifies the input applied to the plant so that its behavior matches the model. MRAC has been applied to the control of a humanoid robot arm driven by McKibben actuators [17], but the authors focus on the behavior of the larger rigid linkage system driven by these

Manuscript received: September, 10, 2016; Revised December, 10, 2016; Accepted January, 2, 2017.

This paper was recommended for publication by Editor Yu Sun upon evaluation of the Associate Editor and Reviewers' comments. This material is based upon work supported by the National Science Foundation under Grant No. IIS-1551219. Any opinions, findings, and conclusions or recommendations expressed in this material are those of the authors and do not necessarily reflect the views of the National Science Foundation.

The authors are with the Mechanical Engineering Department and Robotics Engineering Program, Worcester Polytechnic Institute, MA 01609, USA. All correspondence should be addressed to Cagdas D. Onal cdonal@wpi.edu

Digital Object Identifier (DOI): see top of this page.

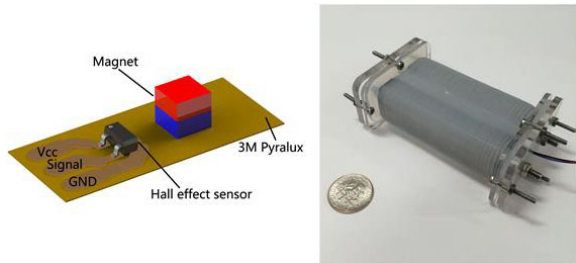


Fig. 1. Our flexible magnetic curvature sensor (a) embedded in our one degree-of-freedom bidirectional bending actuator segment (b).

soft actuators, where the system settling time is only around 10 seconds.

In this article, we seek to combine these two approaches, applying MRAC to the control of soft robotic systems. This is the first time that a model reference adaptive control has been applied to completely soft systems. We focus on the MIT Rule adaptive control, the computationally efficient nature of which allows for easy implementation on embedded hardware. We examine the viability of this MRAC for making different actuators to follow the same linear model tracking rapidly changing and dynamic trajectories (up to 2 Hz), eliminating the need to perform system identification on each new actuator at each driving frequency, range of pressure inputs, or curvature outputs. To validate our approach, we use a feedforward inverse dynamic controller, which uses the reference dynamic model (enforced by the MRAC) to rapidly reach a position. As a result, this paper helps advance soft robot control towards improved repeatability and precision.

II. ACTUATOR DESIGN AND EXPERIMENTAL SETUP

In our previous work [7], we designed a bidirectional soft bending actuation module with integrated proprioceptive curvature sensing. This module, as well as a representation of the curvature sensor, can be seen in Fig. 1. Our custom magnetic curvature sensor utilizes a magnet and a Hall Effect sensor each mounted on a flexible circuit board [18]. The Hall Effect sensor can measure changes in the magnetic field as the position of the magnet changes due to the deformation of the substrate, enabling accurate measurement of the curvature of the system. Our soft bending actuator is comprised of two soft linear muscles [19] and an inextensible constraint layer in between. The individual linear actuators are made of tubes of silicone rubber with engineered cross sections wrapped in inextensible thread, which causes them to extend with minimal radial deformation when pressurized. The constraint layer, with a custom integrated curvature sensor, inhibits this linear extension, resulting in the bending of the entire soft module away from the pressurized actuator. Caps are attached to both ends of the actuator to seal the chambers and allow for modular connections with other segments. The caps are made of two acrylic boards sandwiching the rim of the silicone tube to prevent leaking.

The actuator is driven by two 3-2 (3-port, 2-state) binary solenoid valves, each connecting one pressure chamber to a common 8 psi (55 kPa) pressure source. This pressure value was chosen because it is the highest that the actuators can withstand continuously. The valves can either inflate or deflate a given actuator chamber. We control the pressure in each chamber using a 60 Hz PWM of the valves. We set the valves to operate in complete antagonism, so when one chamber is inflating the other is always deflating. Thus, we can reduce the number of required inputs to one, corresponding to the single (active) degree of freedom (DOF) of the bending actuator. We have previously observed that the valves begin to saturate at duty cycles below 20% or above 80%. Thus, we constrained the duty cycles sent to the system to stay between these two values.

III. SYSTEM IDENTIFICATION

We can treat the dynamic response of the actuator as a generic second-order system:

$$\ddot{x} + a_1\dot{x} + a_2x = bu, \quad (1)$$

where x is the bending angle of the actuator, u is the system control input, and a_1 , a_2 , and b are constant dynamic parameters. The first step in building a reference model for the soft actuator is understanding its nominal performance under full pressure input. To this end, we characterize the values for these constant parameters. We note that this model does not represent the nonlinear system at every pressure input as we have found previously in [12], but only provides a starting point for the reference model.

The general solution of the second order system under constant (step) input is given as:

$$x(t) = C_1e^{(-t/\tau_1)} + C_2e^{(-t/\tau_2)} + C_0 \quad (2)$$

with the boundary conditions $x(t = 0) = 0$ and $\dot{x}(0) = 0$ and where t is time and C_0 , C_1 , C_2 , τ_1 and τ_2 are constants. The relationship between the coefficients in (1) and (2) can be described as follows:

$$\begin{aligned} C_0 + C_1 + C_2 &= 0 \\ C_1/\tau_1 + C_2/\tau_2 &= 0 \\ a_1 &= \frac{1}{\tau_1\tau_2} \\ a_2 &= \frac{1}{\tau_1} + \frac{1}{\tau_2} \\ b &= \frac{1}{\tau_1\tau_2}C_0. \end{aligned} \quad (3)$$

As this is a constant-input solution, u in (3) is constant. We collected the trajectory data from a single actuator using vision tracking software with an input pressure of 8 psi, the maximum pressure applied to the actuator. We fit (2) via least-squares to the resulting dynamic trajectory, yielding time constants $\tau_1 = 0.1107$ and $\tau_2 = 0.0021$ as well as coefficients $C_0 = 0.8366$, $C_1 = -0.8531$, and $C_2 = 0.0165$. To calculate u we assumed that the steady state output of the

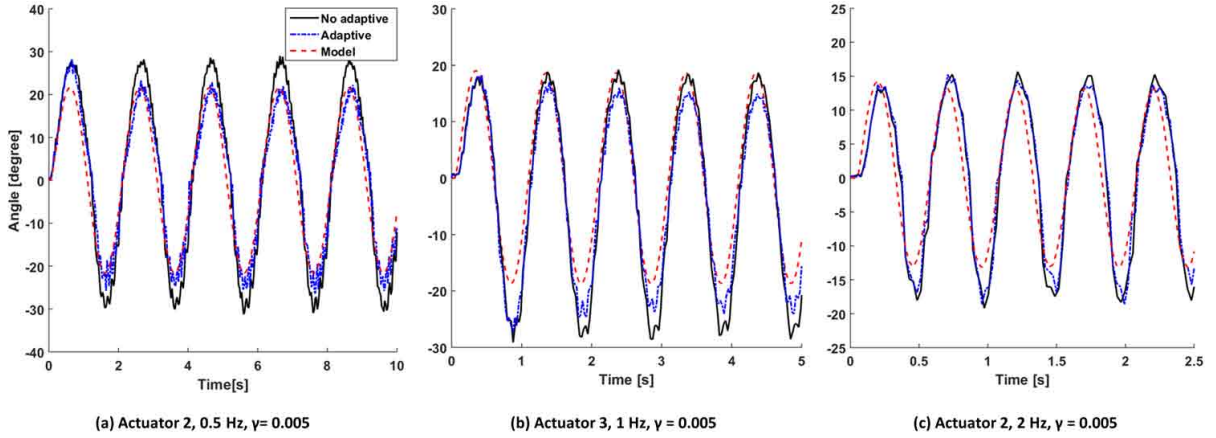


Fig. 2. Three sample trajectories of the system with and without the adaptive control compared to the trajectory of the reference model.

system is a linear function of valve duty cycles between 20% to 80% and that an 80% duty cycle, being fully saturated, is equivalent to 8 psi, the pressure used for the experiment. As 20% would saturate in the opposite direction, and thus be equivalent to 8 psi in the opposite direction, we shifted u for purposes of the dynamic model. Our shifted u varied between -30 and 30 (i.e. $u \in [-30, 30]$). Thus, for system identification in 3, we used $u = 30$. Solving these equations, we get $a_1 = 4221.8$, $a_2 = 476.4912$, and $b = 117.74$.

IV. MODEL REFERENCE ADAPTIVE CONTROLLER

For embedded operation, the MIT rule provides a computationally efficient approach to formulate an MRAC for use with our soft actuators, allowing us to standardize their behavior. This rule introduces an adaptive gain, which changes the system input to match the system behavior to a desired model behavior. The equation translating the nominal input to the system input is as follows:

$$u = u_c \theta + 50 \quad (4)$$

where u_c is the nominal input (bounded between -30 and 30), u is the duty cycle input to the physical system (bounded between 20 and 80), and θ is the adaptive gain. θ is updated at every experimental time step using the following equation:

$$\theta(n) = \theta(n-1) + \gamma(x(n) - x_m(n))x_m(n)\Delta t \quad (5)$$

where x is the position (bending angle) of the actuator, x_m is the position of the actuator model, and Δt is the time step. x_m was calculated using a standard constant-acceleration model over each time step as follows:

$$\ddot{x}_m(n) = -a_{1m}x_m(n) - a_{2m}\dot{x}_m(n) + u_c(n)b_m \quad (6)$$

$$x_m(n+1) = x_m(n) + \dot{x}_m(n)\Delta t + \frac{1}{2}\ddot{x}_m(n)\Delta t^2 \quad (7)$$

$$\dot{x}_m(n+1) = \dot{x}_m(n) + \ddot{x}_m(n)\Delta t \quad (8)$$

where a_{1m} , a_{2m} , and b_m are the system model parameters used in the experiment. Thus, the controller constantly keeps track of the model trajectory and uses it as a reference for the adaptive controller. As we constrained u to remain between 20 and 80, we also saturate u_c to remain within -30 and 30. This prevents the model from being driven in ways the plant is incapable of, which would hinder consistency between the reference model and the experimental plant.

V. INVERSE DYNAMIC CONTROL

We investigated the use of a feed-forward inverse dynamic controller on our system. Using the dynamics of the system model, this controller calculates the control input needed for the system to reach the desired position within a single time step. It does so by first calculating the acceleration required to reach the desired position in a single time step, as shown in the following equation:

$$\ddot{x}_R = \frac{x_d - 2x_m(n) + x_m(n-1)}{\Delta t^2}, \quad (9)$$

where \ddot{x}_R is the required acceleration and x_d is the desired actuator position. This equation is used to calculate the required input to the system by solving (1) for u_c , resulting in the following:

$$u_c = \frac{\ddot{x}_R + a_{1m}x_m + a_{2m}\dot{x}_m}{b_m} \quad (10)$$

Under ideal circumstances this controller, which is entirely open-loop, would allow the system to quickly reach a desired angle. However, since it uses an imperfect model of the system to calculate the required inputs, the feedforward inverse dynamic inputs result in errors in a physical system. We can address this by using the adaptive controller to ensure that the behaviors of the dynamic model and the plant match each other.

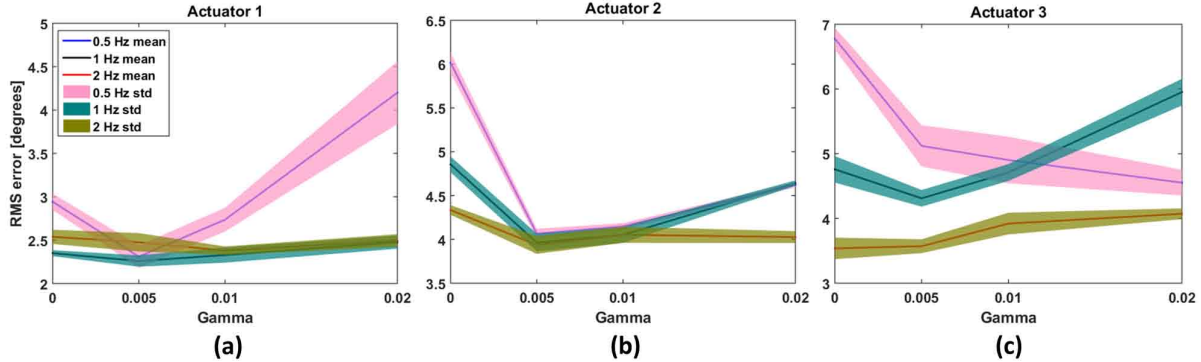


Fig. 3. The mean and standard deviation of the RMS Error between the plant and the reference model.

VI. EXPERIMENTAL RESULTS

For our experiments, we ran our control loop at a constant 1 kHz (thus, $\Delta t = 0.001$). This was set to allow the constant acceleration discretization (6)-(8) to function, as a significantly longer time step would cause the constant-acceleration model to diverge. Because of the nature of the communication link between our computer and the micro-controller, we were unable to relay system information at the control frequency. Thus, data was collected separately at around 40 Hz.

We arbitrarily modified the identified model of the system for use in our experiments. For our reference model we set $a_{1m} = 4000$ and $a_{2m} = 460$. These changes created additional differences between the nominal and desired behavior of the actuator, allowing us to highlight the strength of our approach. The value of b_m varied between the experiments.

In addition, we implemented an initial delay of 50 ms for the model. This was to match a similar delay observed in the behavior of the actuator. The model acceleration in (6) would not be updated until after the first 50 ms of operation, after which it would be updated as normal. This significantly improved the similarity between the plant and the model, as during that period of inaction by the plant θ would increase dramatically, causing significant overshoot at a later point.

A. Model Reference Adaptive Control System Results

Our first experiments involved testing the functionality of the MRAC alone. We applied it under various cases using a sinusoidal input function with amplitude 20 (in modified duty-cycle units) as the input u_c . We collected data in each experiment for 30 seconds and calculated the root-mean-square (RMS) error between the model and the physical system. We performed this experiment three times for each of three actuators, three signal frequencies (0.5, 1, and 2 Hz) and four γ values (0, 0.005, 0.01, and 0.01). The experiments where $\gamma = 0$ represented a control group, where the adaptive controller does not modify the plant behavior. For this experiment, we used $b_m = 80$, instead of the value 117.74 characterized above in Section III. The reduced b_m value helped the continuous dynamic trajectories

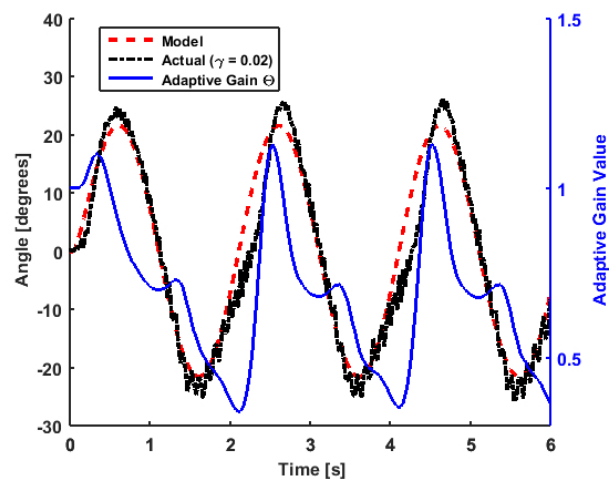


Fig. 4. An example of the behavior of the adaptive gain Θ in (5) during the operation of the Actuator 3. For this plot, the frequency was 0.5 Hz and $\gamma = 0.02$.

of the model be achievable by all of the actuators tested, regardless of any inconsistencies in their fabrication. We had previously observed that higher values of b_m may result in a divergence of θ for actuators that physically cannot provide the desired bending moment under maximum pressure.

Fig. 2 shows three examples of actuator trajectories with and without adaptation, one for each of the frequencies tested for $\gamma = 0.005$. The MRAC has the best results at 0.5 Hz, where it can almost perfectly match the model performance apart from oscillations resulting from valve PWM and sensor noise. It still must adapt within a single cycle, and the adaptive trajectory falls behind and then catches up to the model on the falling component of each period. The advantages are less apparent for 1 Hz, where the adaptive trajectory can not compensate fast enough to match both the peaks and valleys of the trajectory, as the nominal motion of the actuator is skewed in the negative direction. This is likely the result of differences in the material properties or dimensions between each chamber of the actuator, which were fabricated separately. The same is true for the 2 Hz

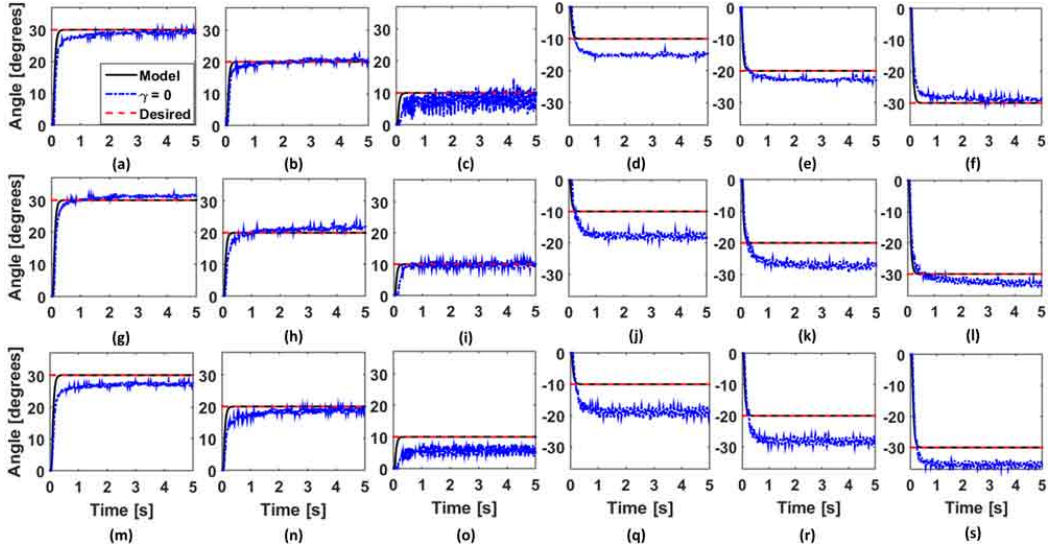


Fig. 5. The results of the open-loop inverse dynamic controller following step functions. (a)-(f) are Actuator 1, (g)-(i) are Actuator 2, and (m)-(s) are Actuator 3.

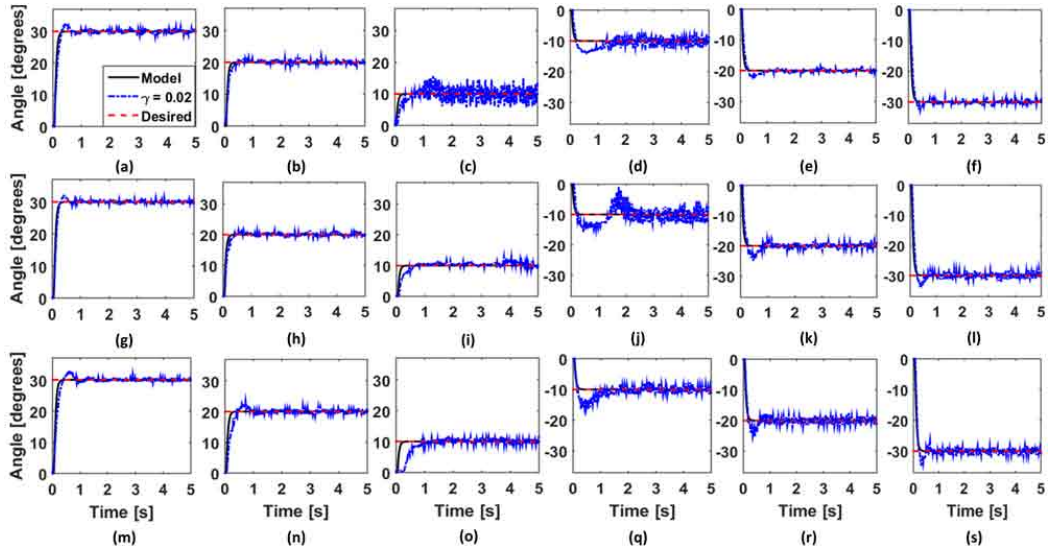


Fig. 6. The results of the inverse dynamic controller augmented by the MRAC ($\gamma = 0.02$) while following step functions. (a)-(f) are Actuator 1, (g)-(i) are Actuator 2, and (m)-(s) are Actuator 3.

signal, where there are only slight benefits to the adaptive control.

We calculated the mean and standard deviation of the RMS errors between the model and actual trajectories for all experiments, as illustrated in Fig. 3. From this figure, we can see that the addition of the proposed adaptive controller resulted in an improvement for at least one value of γ for all experiments except Actuator 3 (Fig. 3-C) at 2 Hz. Overall, $\gamma = 0.005$ provided the most consistent improvement over the actuators and frequencies, though in two cases higher γ values provided additional improvement (Actuator 1 at 2 Hz and Actuator 3 at 0.5 Hz).

We isolated an illustrative example of the behavior of the adaptive gain Θ during actuator operation. We used Actuator

3 at 0.5 Hz using $\gamma=0.02$, the results of this can be seen in Fig. 4. The adaptive gain varies wildly within each sinusoidal cycle, reaching 1.2 while the actuator is in the positive half of its cycle and dropping to 0.3 during the negative half. On the rising part of the signal, a non-linearity in the actuator causes it to lag behind the model, driving the adaptive gain up to compensate. This causes it to slightly overshoot, and the gain drops rapidly to allow the actuator to catch up to the model as it drops.

B. Inverse Dynamic Controller Results

We tested our inverse dynamic feedforward controller against step functions of various bending angles

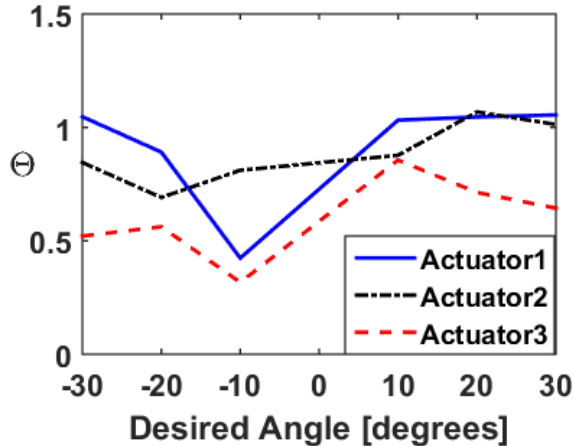


Fig. 7. The steady-state results of θ for the adaptive control augmented inverse dynamic control.

$[30^\circ, 20^\circ, 10^\circ, -10^\circ, -20^\circ, \text{ and } -30^\circ]$ using each of the three actuators. To show the advantages of the adaptive controller, we performed this experiment with and without adaptive control enabled ($\gamma = 0.02$). The higher γ was chosen because, for step references, rapid convergence is desired. We chose $b_m = 100$ as it better matched the identified system model and the application meant we wouldn't risk a divergence of θ . In addition, we observed that using a Δt of 0.001 in (9) would result in too much input saturation. To prevent this, we used $\Delta t = 0.01$ and replaced $x_m(n-1)$ with $x_m(n-10)$, making for a less exacting trajectory, inherently reducing the effect of any noise in sensor measurements. The results of this experiment without adaptation can be seen in Fig. 5 while the results with adaptation can be seen in Fig. 6.

The inverse dynamic controller can quickly reach a desired angle, even when operating without any feedback. However, it does result in some steady-state errors resulting from the differences between the reference model and the physical system. The addition of the MRAC allowed the system to maintain its fast approach while eliminating the steady-state error. We can also observe that the model and the plant behave similarly during the approach to the desired angle, though the plant consistently overshoots before reacquiring the target angle.

One thing we can observe from the non-adaptive trajectories is that the plant has a tendency to drift slowly even after the model input has stabilized. This represents time-variant dynamic behavior which has not been captured by our model. Fortunately, the adaptive controller is able to compensate for it. In addition, we can observe that the steady-state error for the system varies widely with respect to the desired angle. The model actually gets more accurate at higher angles, and the errors are significantly different between the positive and negative sides. This is because the characterization experiment used a constant input in the positive direction that resulted in a large angle, so the model is more accurate in these conditions.

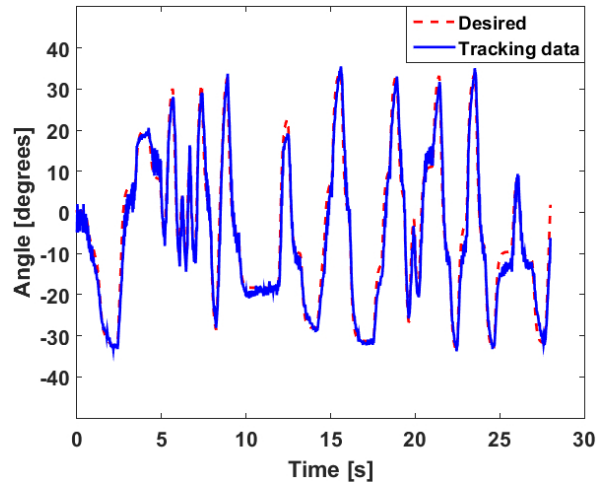


Fig. 8. The behavior of Actuator 1 under user-supplied inputs. MRAC was used with $\gamma = 0.005$.

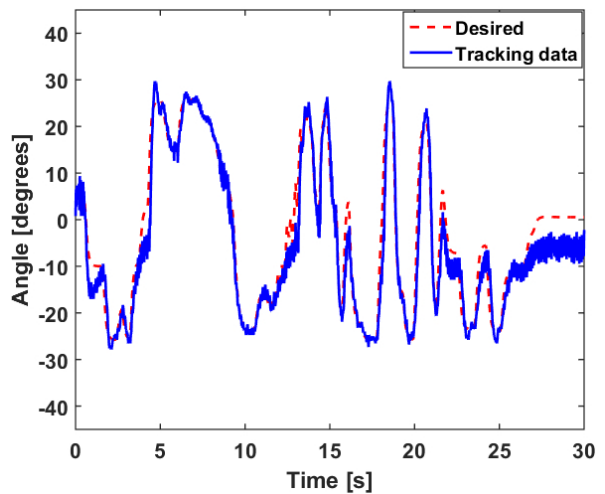


Fig. 9. The behavior of Actuator 1 under user-supplied inputs. MRAC was used with $\gamma = 0.02$.

We also recorded the steady state value of the adaptive gain θ for each experiment in Fig. 6. This was done by taking the mean of the last 20 data points for each experiment after convergence is observed, and its results can be seen in Fig. 7. As every experiment converged to the angle specified by the model, these differences in θ provide a visual representation of the nonlinearities in the actuator dynamics, as well as the variation between the behavior of different soft bending actuators.

C. Unstructured Signal Tracking

Our final experiment was to investigate the performance of the adaptive controller in tracking unstructured continuous references. We connected a user input knob to the embedded controller and mapped its positions to system inputs between -30° and 30° . A user manipulated the knob, and the system responded to the input while the MRAC worked to try and

keep the system in sync with the model. Results of these trials can be seen in Fig. 8 with $\gamma = 0.005$ and Fig. 9 for $\gamma = 0.02$.

Results show that the model and the system behave similarly, even under the unstructured inputs. We can see the effect of the lower γ , as in Fig. 8 the system does not respond fast enough to reach some of the peaks the model does. In addition, we can observe that the adaptive controller has difficulty matching the system to the model when the model is around 0. This is because of the x_m term in the adaptive update equation in (5) indicates that when the model output is near zero, θ will be updated slowly. Our control method requires the valves to be constantly operating, with an equal 50% duty cycle for each valve supposedly corresponding to an angle of 0. Unfortunately, differences between our actuators can cause this state to have a slight bias (for this actuator, in the negative direction), something the MIT rule adaptive MRAC is unable to compensate for.

VII. CONCLUSION

In this paper we formulated a model reference adaptive controller to ensure that our soft pneumatic bending actuators exhibit a behavior that is uniformly consistent with that of a linear system model. We developed and characterized a simple linear dynamic model of our actuator, which served as a basis for our reference model. We applied our MRAC to a range of actuators under a range of frequencies and adaptive update gains. We found that small update gains allowed for increased performance in model following, while larger gains would sometimes cause degradations in performance. In addition we used the dynamic actuator model to develop a feed-forward inverse dynamic controller for our actuator to augment the adaptive controller to ensure accurate position control of soft pneumatic actuators. We tested this controller on different actuators against step functions of various amplitudes and achieved successful tracking. Finally, we used unstructured inputs from a user to provide reference positions for the actuator to track, demonstrating the versatility of the proposed control approach.

We observed that the adaptive gain θ converged to very different results depending on where in the workspace the desired position was located. In particular, it approached different values depending on if the actuator was bending in positive or negative directions. This is likely the result of differences between the two pressure chambers which were molded separately and then attached together to form the full actuator. When γ is high, it causes the actuator to over fit a single half-cycle, resulting in worse performance for the other half-cycle. This is why increases in γ can cause a degradation in performance.

We would like to expand this work into a series of actuators mounted together to form a soft pneumatic tentacle, each actuator running the same inverse-dynamic feedforward augmented MRAC. This approach will ensure that each module behaves as desired, allowing the soft tentacle to

predictably perform manipulation tasks, such as squeezing into tight spaces and grasping objects therein.

REFERENCES

- [1] Y.-L. Park, S. J. G. K. E. C. Goldfield, and W. R.J. "A soft wearable robotic device for active knee motions using flat pneumatic artificial muscles," in *Robotics and Automation (ICRA), 2014 IEEE International Conference on*, pp. 4805–4810, IEEE, 2014.
- [2] F. Renda, M. Cianchetti, M. Giorelli, A. Arienti, and C. Laschi, "A 3d steady-state model of a tendon-driven continuum soft manipulator inspired by the octopus arm," *Bioinspiration & biomimetics*, vol. 7, no. 2, p. 025006, 2012.
- [3] A. D. Marchese, C. D. Onal, and D. Rus, "Autonomous soft robotic fish capable of escape maneuvers using fluidic elastomer actuators," *Soft Robotics*, vol. 1, no. 1, pp. 75–87, 2014.
- [4] R. F. Shepherd, F. Ilievski, W. Choi, S. A. Morin, A. A. Stokes, A. D. Mazzeo, X. Chen, M. Wang, and G. M. Whitesides, "Multigait soft robot," *Proceedings of the National Academy of Sciences*, vol. 108, no. 51, pp. 20400–20403, 2011.
- [5] B. A. Trimmer, H.-T. Lin, A. Baryshyan, G. G. Leisk, and D. L. Kaplan, "Towards a biomorphic soft robot: design constraints and solutions," in *2012 4th IEEE RAS & EMBS International Conference on Biomedical Robotics and Biomechanics (BioRob)*, pp. 599–605, IEEE, 2012.
- [6] M. Luo, Y. Pan, E. Skorina, W. Tao, F. Chen, S. Ozel, and C. Onal, "Slithering towards autonomy: a self-contained soft robotic snake platform with integrated curvature sensing," *Bioinspiration & biomimetics*, vol. 10, no. 5, pp. 055001–055001, 2015.
- [7] M. Luo, E. H. Skorina, W. Tao, F. Chen, S. Ozel, Y. Sun, and C. D. Onal, "Towards modular soft robotics: Proprioceptive curvature sensing and sliding-mode control of soft bidirectional bending modules," *Soft Robotics*, 2016.
- [8] B. Trimmer, "Soft robot control systems: A new grand challenge?," *Soft Robotics*, vol. 1, 2014.
- [9] J. C. Case, E. L. White, and R. K. Kramer, "Soft material characterization for robotic applications," *Soft Robotics*, vol. 2, no. 2, pp. 80–87, 2015.
- [10] Y. Sun, Y. S. Song, and J. Paik, "Characterization of silicone rubber based soft pneumatic actuators," in *Intelligent Robots and Systems, 2013. IEEE/RSJ International Conference on*, pp. 4446–4453, IEEE, 2013.
- [11] H. Zhao, R. Huang, and R. F. Shepherd, "Curvature control of soft orthotics via low cost solid-state optics," in *2016 IEEE International Conference on Robotics and Automation (ICRA)*, pp. 4008–4013, IEEE, 2016.
- [12] E. H. Skorina, M. Luo, S. Ozel, F. Chen, W. Tao, and C. D. Onal, "Feedforward augmented sliding mode motion control of antagonistic soft pneumatic actuators," in *Robotics and Automation (ICRA), 2015 IEEE International Conference on*, pp. 2544–2549, IEEE, 2015.
- [13] P. Polygerinos, Z. Wang, J. T. Overvelde, K. C. Galloway, R. J. Wood, K. Bertoldi, and C. J. Walsh, "Modeling of soft fiber-reinforced bending actuators," *IEEE Transactions on Robotics*, vol. 31, no. 3, pp. 778–789, 2015.
- [14] N. Farrow and N. Correll, "A soft pneumatic actuator that can sense grasp and touch," in *Intelligent Robots and Systems, 2015. IEEE/RSJ International Conference on*, pp. 2317–2323, IEEE, 2015.
- [15] C. Onal and D. Rus, "Autonomous undulatory serpentine locomotion utilizing body dynamics of a fluidic soft robot," *Bioinspiration and Biomimetics*, vol. 8, no. 2, 2013.
- [16] C.-c. Hang and P. Parks, "Comparative studies of model reference adaptive control systems," *IEEE transactions on automatic control*, vol. 18, no. 5, pp. 419–428, 1973.
- [17] G. Tonietti and A. Bicchi, "Adaptive simultaneous position and stiffness control for a soft robot arm," in *Intelligent Robots and Systems, 2002 IEEE International Conference on*, pp. 1992–1997, IEEE, 2002.
- [18] S. Ozel, N. Keskin, D. Khea, and C. Onal, "A precise embedded curvature sensor module for soft-bodied robots," *Sensors and Actuators A: Physical*, vol. 236, pp. 349–356, 2015.
- [19] M. Luo, E. Skorina, W. OO, W. Tao, F. Chen, S. Youssefian, N. Rahbar, and C. Onal, "Reverse pneumatic artificial muscles (rpams): Modeling, integration, and control," *PLOS One*, 2016 (under review).